The Effects of Varying Salinity on Ammonium Exchange in Estuarine Sediments of the Parker River, Massachusetts

Nathaniel B. Weston · Anne E. Giblin · Gary T. Banta ·
Charles S. Hopkinson · Jane Tucker

Abstract We examined the effects of seasonal salinity changes on sediment ammonium (NH_4^+) adsorption and exchange across the sediment–water interface in the Parker River Estuary, by means of seasonal field sampling, laboratory adsorption experiments, and modeling. The fraction of dissolved NH_4^+ relative to adsorbed NH_4^+ in oligohaline sediments rose significantly with increased pore water salinity over the season. Laboratory experiments demonstrated that small (~3) increases in salinity from freshwater conditions had the greatest effect on NH_4^+ adsorption by reducing the exchangeable pool from 69% to 14% of the total NH_4^+ in the upper estuary sediments that experience large (0–20) seasonal salinity shifts. NH_4^+ dynamics did not appear to be significantly affected by salinity in sediments of the lower estuary where salinities under 10 were not measured. We further assessed the importance of salinity-mediated desorption by constructing a simple mechanistic numerical model for pore water chloride and NH_4^+ diffusion for sediments of the upper estuary. The model predicted pore water salinity and NH_4^+ profiles that fit measured profiles very well and described a seasonal pattern of NH_4^+ flux from the sediment that was significantly affected by salinity. The model demonstrated that changes in salinity on several timescales (tidally, seasonally, and annually) can significantly alter the magnitude and timing of NH_4^+ release from the sediments. Salinity-mediated desorption and fluxes of NH_4^+ from sediments in the upper estuary can be of similar magnitude to rates of organic nitrogen mineralization and may therefore be important in supporting estuarine productivity when watershed inputs of N are low.

Keywords Sediments · Ammonium · Adsorption · Parker River estuary · Salinity · Estuary

N. B. Weston (✉)
Department of Geography and the Environment,
Villanova University,
Villanova, PA, USA
e-mail: nathaniel.weston@villanova.edu

A. E. Giblin · J. Tucker
The Ecosystems Center, Marine Biological Laboratory,
Woods Hole, MA, USA

G. T. Banta
Department of Environmental, Social, and Spatial Change,
Roskilde University,
Roskilde, Denmark

C. S. Hopkinson
Department of Marine Sciences, University of Georgia,
Athens, GA, USA

Introduction

Nitrogen dynamics are important in determining the levels and patterns of estuarine productivity, as primary production in many coastal systems is generally nitrogen-limited (Howarth 1988). Benthic nitrogen biogeochemistry is a critical component of estuarine nitrogen cycling. Sediments can be a source of inorganic nitrogen to support estuarine primary production through benthic organic matter decomposition (Nixon 1981; Boynton and Kemp 1985; Giblin et al. 1997; Hopkinson et al. 1999). A significant portion of remineralized N can also be removed from the system as dinitrogen gas through coupled nitrification–denitrification in the benthos (Seitzinger 1988; Sorensen and Jørgensen 1987).

Salinity can influence benthic nitrogen cycling in a number of ways. Ammonium (NH_4^+) flux from freshwater sediments is typically very low compared to saline sedi-

ments, even when mineralization rates are comparable (Mortimer 1971; Boatman and Murray 1982; Seitzinger 1988; Gardner et al. 1991; Rysgaard et al. 1999). The lower activity of other ions in freshwater allows greater adsorption of NH_4^+ onto particle exchange sites (Rosenfeld 1979; Boatman and Murray 1982; Seitzinger et al. 1991). Competition for exchange sites by other ions in saline waters (Seitzinger et al. 1991), as well as ion pairing of NH_4^+ with anions in saline water (Gardner et al. 1991), reduces storage of NH_4^+ in saline sediments. NH_4^+ in sediments exists in equilibrium between the exchangeable and dissolved pools, where the amount of exchangeable NH_4^+ is regulated by the pore water NH_4^+ concentration, the exchange capacity of the sediment, and the concentration and equilibrium reactions of other ions in the sediment (Berner 1980).

Salinity can also affect N cycling in sediments by influencing microbes that mediate nitrification and denitrification (Seitzinger 1988; Rysgaard et al. 1999). Nitrification, the conversion of NH_4^+ to nitrate (NO_3^-), has been shown to be inhibited by sulfide production in saline sediments (Joye and Hollibaugh 1995), and there is evidence for direct physiological effects of salts on nitrifiers and denitrifiers (Finstein and Bitzky 1972; Rysgaard et al. 1999; Mondrup 1999). Therefore, salinity can further enhance NH_4^+ release from sediments through inhibition of nitrification–denitrification (Seitzinger et al. 1991).

Nitrogen cycling may be especially influenced by salinity in sediments that are periodically fresh and experience substantial changes in salinity. Several studies have documented higher ammonium exchange capacity of freshwater sediments (Seitzinger et al. 1991; Morlock et al. 1997; Simon and Kennedy 1987). Hopkinson et al. (1999) measured higher than expected NH_4^+ flux from sediments in the oligohaline reach of the Parker River estuary during periods of low freshwater discharge and high salinity. Rysgaard et al. (1999) found increased benthic NH_4^+ flux and decreased nitrification and denitrification as salinity increased, with the most significant effects between 0 and 10.

Salinity-driven desorption and subsequent flux of NH_4^+ from sediments are possible sources of inorganic nitrogen for primary production in estuaries. Holmes et al. (2000), in a study of the upper Parker River estuary, noted a decoupling of the timing of phytoplankton blooms and nutrient inputs from the watershed and concluded that benthic recycling provided the majority of inorganic nitrogen for primary producers when freshwater inputs (and external nutrient inputs) were low. Hopkinson et al. (1999) hypothesized that salinity-driven desorption in the upper Parker River estuary was a mechanism supporting primary production at times when watershed N inputs were low.

In this study, we investigated the effects of salinity changes on sediment NH_4^+ adsorption through laboratory experiments and seasonal sampling in the Parker River estuary. Furthermore, we created a simple model to assess the relative importance of salinity-driven desorption to benthic NH_4^+ flux rates. Benthic metabolism and nitrogen fluxes as well as rates of denitrification and dissimilatory nitrate reduction to ammonium were measured in the Parker River and are described in Giblin et al. (2010). The upper reaches of the Parker River estuary can experience large seasonal (0–25) changes in salinity and support large standing stocks of chlorophyll *a* when nutrient inputs from the watershed are low (Wright et al. 1987; Hopkinson et al. 1999; Holmes et al. 2000). We hypothesized that when nitrogen inputs from the watershed decreased and estuarine salinity increased during the summer, salinity-driven desorption and flux of benthic NH_4^+ into the overlying water provided a source of inorganic nitrogen to primary producers in the estuary. We also hypothesized that NH_4^+ flux may be influenced by estuarine salinity regimes on daily (tidal), seasonal (high- versus low-discharge times of year), and annual (differences between water years) timescales and used the model to address these questions. The processes of salinity-driven desorption and subsequent flux of NH_4^+ from sediments may have implications for temporal patterns in N cycling and productivity in estuaries with tidal, seasonal, and/or annual changes in salinity.

Materials and Methods

Site Description and Water Column Measurements

This study was conducted in the Parker River, Plum Island Sound, estuarine system on the northern coast of Massachusetts (Fig. 1). This site is part of the Plum Island Ecosystem Long-Term Ecological Research project (http://www.mbl.edu/PIE). Freshwater input to the estuary from the Parker River averages 1.1 $m^3 s^{-1}$ annually and is markedly seasonal, averaging 2.1 $m^3 s^{-1}$ during spring (Mar–May) and 0.4 $m^3 s^{-1}$ during summer (Jun–Aug). Salinities in the upper estuary are dependant on the freshwater discharge and can range from 0 for several kilometers below the dam during times of high flow to above 20 at the dam in late summer. The 24-km estuary has a semidiurnal macrotidal cycle, with an average tidal range of 2.9 m. Tidal salinity oscillations can be as high as 12 in the mid and upper estuary. Vallino and Hopkinson (1998) describe the hydrology of the Parker River estuary in detail.

We sampled five sites in the Parker River estuary, Plum Island Sound system, that represented the down-estuary gradient of salinity and sediment type during 1999 (Fig. 1, Table 1). Sites P24 and P22 (0 and 1.7 km downstream of

Fig. 1 The Parker River/Plum Island Sound estuarine system with the five benthic sampling sites indicated. The location of the study domain on the northern coast of Massachusetts is indicated in the *inset map*
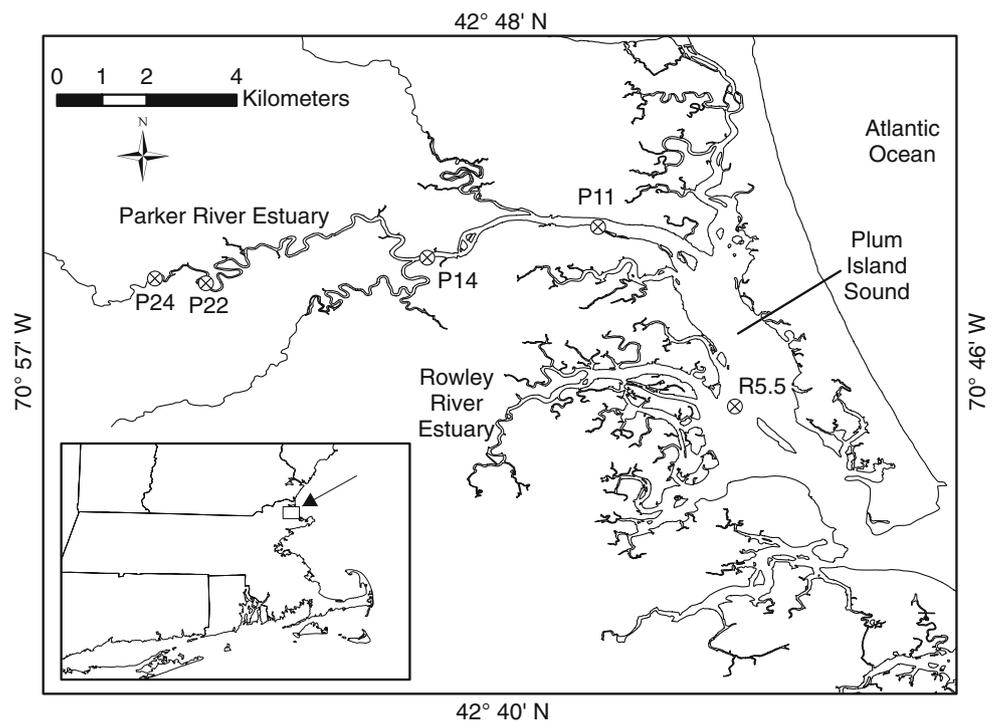
the dam, respectively), in the upper reaches of the Parker River estuary, were characterized by fine silt and clay sediments. Sites P14 and P11 (10 and 13 km) represented the mid to lower region of the Parker River estuary, with coarser muds and fine sand. The R5.5 station (18.5 km) at the mouth of the Rowley River Estuary was a sandy saline site. Benthic metabolism and nutrient cycling were measured by Hopkinson et al. (1999) at sites P22 (called P2 in that paper), P14 (called P5), and R5.5 (called Rowley) in 1993 and 1994 and at site P22 by Giblin et al. (2010) in 1993–2006.

Temperature and salinity were recorded every half hour at site P22 from March 18 through July 22 with a Hydrolab DataSonde 4 and July 22 through November 11 with a YSI 6600 DataSonde during 1999. Sonde salinity calibration was checked at least every 3 weeks and recalibrated as needed.

Discharge from the Parker River is monitored by the USGS (http://www.usgs.gov, station 01101000). Inorganic nitrogen loading to the estuary was calculated from discharge and NH_4^+ and NO_3^- concentrations at the Parker Dam (Fig. 1). Nutrient samples were collected at the dam

Table 1 Benthic sampling site locations and sediment type, porosity, bulk density, salinity, organic carbon, carbon to nitrogen ratios, and adsorption coefficients

Site	P24	P22	P14	P11	R5.5
Distance from dam (km)	0.1	1.7	10	13	18.5
Distance from mouth (km)	23.9	22.3	14	11	5.5
Sediment type	Fine mud	Fine mud	Fine sand/mud	Fine sand/mud	Sand
Sediment porosity (g cm^{-3})[a]	0.76±0.02	0.72±0.01	0.60±0.01	0.49±0.01	0.43±0.01
Sediment bulk density (g cm^{-3})[a]	0.58±0.02	0.63±0.01	1.04±0.03	1.38±0.03	1.51±0.03
Salinity range	0–20	0–20	5–34	10–34	13–34
Sediment % carbon[b]	3.68±0.12	3.77±0.21	1.73±0.19	0.41±0.07	0.14±0.04
Sediment C/N[b]	14.67	15.02	16.43	14.11	7.43
K' (ml g^{-1})	2.8	1.7	0.7	0.8	0.9
R^2 of K' isotherm	0.69	0.70	0.72	0.42	0.19
K	3.2	2.2	2.6	4.4	7.6

[a] Top 10 cm of sediment, n=30-54±SE; [b] n=12-15±SE

periodically from 1993 through 2001, filtered (GF/F), and frozen until analysis. NH_4^+ was determined using the phenol hypochlorite method (Solorzano 1969). NO_3^- was analyzed using the cadmium reduction method on an autoanalyzer (Alpkem RFA-300 or Lachat Quick-Chem 8000).

Estuarine water column chlorophyll a and NH_4^+ samples were collected periodically from 1994 through 2001. NH_4^+ was determined as previously described. Water samples for chlorophyll a were filtered onto GF/C glass fiber filters, stabilized with $MgCO_3$, and frozen until analysis. Samples were analyzed fluorometrically before and after acidification following overnight extraction in cold acetone (Strickland and Parsons 1972).

Salinity and Nitrogen Pool Surveys

Sediment cores were obtained on seven dates in 1999 at the five sites in Plum Island and on three additional dates at site P22 only. At sites P24, P22, and P14, 6.5-cm-diameter sediment cores were taken for pore water and exchangeable NH_4^+ and 3.3-cm-diameter cores for porosity, bulk density, and C/N analysis. At P11 and R5.5, all collections were made with the 3.3-cm-diameter cores. Cores from P24, P22, and P14 were sectioned and analyzed the day following collection. We found it necessary to freeze cores from P11 and R5.5 before sectioning, as these sandy sediments drained easily and were difficult to section without freezing.

Sediment cores were sectioned in 1-cm intervals from 0 to 2 cm, 2-cm intervals to 10 cm, and 4-cm intervals below 10 cm. For 6.5-cm-diameter cores, one core was used for both pore water and exchangeable NH_4^+ analysis, while two duplicate 3.3-cm cores were used for separate analysis for sediments from the P11 and R5.5 stations. Duplicate 6.5-cm cores were sectioned from site P22 for both pore water and exchangeable NH_4^+ on all dates. On one date (April 12), analyses were completed in duplicate for stations P24, P14, P11, and R5.5 and in triplicate for site P22. Duplicates varied by less than approximately 10% for salinity, pore water NH_4^+, and exchangeable NH_4^+.

Sediment sections for pore water NH_4^+ and salinity were centrifuged for 10 min at 7,000 rpm and analyzed with the phenol hypochlorite method, modified for small sample size (Solorzano 1969). Sediments from P11, R5.5, and bottom sections of P14 were centrifuged in split centrifuge tubes, in which pore water was forced through a GF/D glass fiber filter. Pore water salinity was determined using a Reichert refractometer. Chlorinity on a subset of samples ($n=19$) from various dates, depths, and sites was analyzed on a Dionex DX-120 ion chromatograph. Chlorinity was converted to salinity and compared to refractometer readings. Agreement was good between the

refractometer and the chromatograph (slope=1.14, $R^2=0.99$, data not shown).

Exchangeable NH_4^+ was determined with a 2 N KCl extraction (Rosenfeld 1979). Sediment sections were mixed with 2 N KCl in approximately 3:1 w/w KCl to wet sediment ratios and placed on a shaker table for 1 h. The KCl extract was then analyzed for NH_4^+ (Solorzano 1969). To validate that we were removing all of the exchangeable NH_4^+ with extractions in a 3:1 ratio (e.g., Morin and Morse 1999), we extracted a subset of sediment from site P22 with 2 N KCl in a 50:1 w/w ratio and found no significant difference between extraction methods ($\pm10\%$).

The pore water and exchangeable NH_4^+ adsorption data were used to determine the adsorption coefficients K' ($\mu mol\ N g^{-1} mM^{-1}$) and K (unitless). The slope of the relationship between dissolved (mM) and exchangeable ($\mu mol\ g^{-1}$) NH_4^+ was determined using all data from each site to calculate K' (Mackin and Aller 1984). These values were then converted to K by multiplying K' by the ratio of percent sediment to percent water (Rosenfeld 1979; Mackin and Aller 1984). K' was also determined for site P22 using all pore water and exchangeable NH_4^+ measurements on a single data point basis.

Sediment porosity and bulk density were determined by weight loss of sediment after drying at 90°C overnight. Selected samples of dried sediment were saved for later analysis on a Perkin Elmer 2400 CHN Elemental Analyzer for carbon and nitrogen content. Surface sediments (0–2 cm) and sediments at depth (10–14 cm) from each of the five sites on five dates were analyzed after carbonate removal. Carbonates were removed by fuming moist sediment over concentrated HCl for 3 days. Sediment C and N content was corrected for weight change due to carbonate removal.

Laboratory Adsorption Experiment

The relationship between exchangeable and dissolved NH_4^+ and salinity was determined in the laboratory for sediment from site P22. This site was chosen due to the relatively large seasonal differences in salinity driven by river discharge observed at this site and because of previous data on N cycling processes measured at this site (Hopkinson et al. 1999; Giblin et al. 2010). Sediment was collected from the top 10 cm at site P22, homogenized, and sieved (2 mm). The exchangeable and pore water NH_4^+ was removed from the sediment with repeated 2 N KCl extractions, until no NH_4^+ was detectable in the extractant. The sediment was then split into four equal volumes processed as follows to achieve four treatment levels of pore water salinity: 0, 3, 10, and 34. After water of the desired salinity was added, the sediment was shaken for 1 h

and centrifuged, and the supernatant was removed. This rinsing process was repeated three times, such that the desired salinity was measured in the supernatant of each treatment.

Sediment from each salinity treatment was then split into ten centrifuge tubes (approximately 2 g each) and 10 ml of the appropriate salinity water added. Varying amounts of a NH_4Cl stock solution were added to the sediment slurries, yielding final nominal concentrations of approximately 100, 200, 500, 1,000, and 2,000 μM NH_4^+, in duplicate for each salinity treatment. The sediment was then shaken overnight. A portion of sediment was also dried at 100°C for porosity determination. After overnight equilibration, the sediments were centrifuged, and dissolved NH_4^+ was measured in the supernatant. To make a 2 N KCl solution, 1.5 g KCl was then added to each tube. The tubes were shaken for 1 h, and NH_4^+ was measured again after centrifuging. K' and K were determined for each salinity treatment separately as described previously.

Salinity Diffusion and Nitrogen Exchange Model

A simple one-dimensional mechanistic model of pore water chloride diffusion was created in which we estimated numerically the changes in concentration and flux of chloride according to the equations of Boudreau (1997):

$$\frac{\partial C_{Cl^-}}{\partial t} = \frac{\partial}{\partial z}\left(\varphi D'_{Cl^-}\frac{\partial C_{Cl^-}}{\partial z}\right) \qquad (1)$$

where C_{Cl^-} is the concentration of chloride (μmol cm^{-3}), t is time (seconds), φ is the sediment porosity, D'_{Cl^-} is the sediment diffusion coefficient for chloride (cm^{2}s^{-1}), and z is depth (cm). D'_{Cl^-} was derived from the molecular diffusion constant $D^o_{Cl^-}$ by the relationship $D'_{Cl^-} = D^o_{Cl^-}\left[1 - \ln(\varphi)^2\right]^{-1}$. $D^o_{Cl^-}$ is temperature dependant, and $D^o_{Cl^-}$ (10^{-6}cm s^{-1}) was determined using the linear regression $D^o_{Cl^-} = 0.438(T) + 9.60$, where T is temperature (°C; Boudreau 1997).

The model used 0.5-cm sections to a depth of 40 cm and 0.5-h time steps. Chloride concentrations were calculated explicitly based on the previous time step. The measured pore water chloride profile from March was used as the initial condition, and the average daily overlying water salinity (converted to chlorinity by multiplying by 0.0157) was used as the model driver. The model was constructed such that there was no flux allowed across the bottom boundary. A seasonally smoothed temperature curve (Fig. 3) was used in determining $D^o_{Cl^-}$ (Fig. 3, $T = -1.507(10^{-3})x^2 + 0.6026x - 35.15$, in degrees Celsius where x is Julian day).

The pore water chloride diffusion model was then incorporated into a nitrogen exchange model similar to the chloride diffusion model:

$$\frac{\partial \widehat{C}_{NH_4^+}}{\partial t} = \frac{\partial}{\partial z}\left(\varphi D'_{NH_4^+}\frac{\partial C_{NH_4^+}}{\partial z}\right) + R \qquad (2)$$

where $\widehat{C}_{NH_4^+}$ is the total sediment NH_4^+ concentration (μmol cm^{-3}), $D'_{NH_4^+}$ is the effective NH_4^+ diffusion coefficient, and R is the net benthic production of NH_4^+. The dissolved NH_4^+ concentration, $C_{NH_4^+}$ (μmol cm^{-3}), was determined as a function derived from the relationship between the pore water and total NH_4^+ at varying salinities at site P22. C_{Cl^-} from the chloride diffusion model (Eq. 1) at the appropriate depth and time was used to determine the distribution of the total NH_4^+ between exchangeable and pore water pools. Desorption was assumed to be rapid in relation to the time steps of the model. The measured total NH_4^+ profile from March was used as the starting condition for $\widehat{C}_{NH_4^+}$. Temperature dependence of the NH_4^+ diffusion coefficient $D^o_{NH_4^+}$ (10^{-6}cm^{2}s^{-1}) was calculated as $D^o_{NH_4^+} = 0.413(T) + 9.50$ (Boudreau 1997). For the purposes of describing the NH_4^+ gradient between the top sediment section and the overlying water, water column NH_4^+ concentration was assumed to be constant at 3 μM based on average NH_4^+ concentrations in the upper Parker River Estuary (2.6 μM±2.7 SD, n=264).

The net NH_4^+ production, R, was based on estimated production of NH_4^+ within the sediments minus loss of NH_4^+ through coupled nitrification–denitrification. These data are derived from Giblin et al. (2010), who measured benthic metabolism, nutrient fluxes, and denitrification at site P22 on five dates in 1999. Briefly, benthic fluxes were measured on six sediment cores (15-cm diameter) collected from site P22 and incubated at ambient temperatures. Four of these cores were used for measurements of both direct denitrification and coupled nitrification–denitrification using the ^{15}N isotope pairing technique (Nielsen 1992) while two cores did not receive ^{15}N amendments. Measured benthic nitrate + nitrite (NO$_x$) fluxes at site P22 on these five dates (−0.02± 0.12 mmol m^{-2} day^{-1}; Giblin et al. 2010) indicate net NO$_x$ uptake at this site and therefore no loss of NH_4^+ through efflux of NO$_x$ following nitrification. NH_4^+ remineralization within the sediments was estimated from measured dissolved inorganic carbon fluxes (from Giblin et al. 2010), assuming that the organic matter undergoing mineralization had a C/N ratio of 12.7. This C/N ratio was chosen as a value between the bulk sediment C/N of 15.7 at site P22 (Table 1) and a C/N of 6.6 for phytoplankton (Redfield 1958), though note that an analysis of model sensitivity to variations in the C/N ratio was conducted (*see below*). Net NH_4^+ production was

seasonally smoothed, so that R fits the polynomial equation $R(\text{mmol m}^{-2}\text{day}^{-1}) = 1.3627(10^{-8})x^4 - 1.0579(10^{-5})x^3 + 2.7141(10^{-3})x^2 - 0.25812x + 9.01$, where x is Julian day (valid from 18 March to 10 November only). NH_4^+ production was assumed to be highest in the near-surface sediments and decrease exponentially with depth ($R = 0.95e^{-0.2z}$, where z is depth in centimeters; see below for further discussion), and denitrification was assumed to occur entirely within the top 4 cm (Hartnett and Seitzinger 2003).

Data from a benthic flux core incubation experiment in May 2000 were used to validate the salinity diffusion and nitrogen exchange models. In the experiment, benthic flux cores (15-cm diameter) from site P22 were incubated for 7 days with overlying water of two salinities; 0 (in situ) and 8, in replicate. NH_4^+ concentration was monitored in the overlying water several times during the experiment, and the water was replaced once on day 5 to alleviate NH_4^+ buildup in the overlying water. At the termination of the experiment, the sediment cores were sectioned, and pore water NH_4^+ concentration was determined. Experimental design and methodology for the benthic fluxes are described in more detail in Giblin et al. (2010). Sediment profiles of total NH_4^+ and salinity were determined on separate initial cores, and these data were used as the initial conditions for the models. The models were run as described previously, modifying only the bottom boundary condition to match the depth of the core (20 cm), setting the net NH_4^+ production rate at 3.9 mmol m^{-2} day^{-1} (based on a DIC flux rate of approximately 50 mmol m^{-2} day^{-1} (see Giblin et al. 2010) and a C/N ratio of 12.7), and allowing the NH_4^+ flux across the sediment–water interface to accumulate in the overlying water.

A sensitivity analysis was conducted to determine the response of the nitrogen exchange model to changes in the magnitude and depth distribution of nitrogen cycling processes. The model was run with rates of denitrification halved (scenario B) and doubled (scenario C) relative to rates in the base model (scenario A). Nitrogen remineralization rates were also halved (scenario D) and doubled (scenario E) relative to base model rates. All other parameters were kept at base model values. Further sensitivity analyses were performed by holding the denitrification and remineralization rates constant (at base model values) and varying only the depth distribution of net NH_4^+ production, R. Three scenarios (F–H) were created, with differing rates of exponential decrease of the fraction of R with depth and increasing relative importance of R in the deeper sediments. The equation for the depth distribution of R with depth was $R = \alpha e^{-kz}$, where α is fractional rate of R at the sediment–water interface and k is the extinction coefficient of the R distribution with depth z. The base model value of k (0.2; scenario A) was changed to 1.0

(scenario F), 0.5 (scenario G), and 0.05 (scenario H) with corresponding α values of 0.10 (A), 0.39 (F), 0.22 (G), and 0.03 (H). These four scenarios result in depths of 22.1 cm (A), 4.4 cm (F), 8.8 cm (G), and 38.2 cm (H), respectively, above which 99% of R occurred.

A second set of simulations were run using four different seasonal salinity regimes: a "normal" year, a "dry" year, a "wet" year, and a year in which the water column stayed entirely fresh. The normal-year salinity regime was based on the 56-year average discharge record from the Parker River (USGS station 01101000) and the advection–dispersion model constructed by Vallino and Hopkinson (1998) for the Parker River estuary. The seasonal salinity was smoothed and somewhat idealized but adequately represents the salinity at site P22 in a "normal" water year. In the dry year, salinity was increased at site P22 a month earlier and reached a higher maximum salinity. A hypothetical midsummer rain event in the wet year flushed the saline water from the estuary, keeping salinities low such as those that occurred in 2004. The nitrogen exchange model was run with the same parameters as in previous runs, changing only the overlying water salinity. A final simulation was created that incorporated tidal salinity oscillations by using measured salinities at site P22 (measured every half hour), rather than the average daily salinities used in previous model runs.

Results

Water Column Measurements

Seven years of loading measurements to the Parker River estuary showed high inorganic nitrogen inputs during the winter–spring period and consistently low inputs during the summer (Fig. 2a). Conversely, chlorophyll a concentrations in the upper estuary were typically highest in the summer and fall (Fig. 2a). Chlorophyll a was significantly higher during periods of lower nitrogen loading from the river (Fig. 2b).

Water column salinity and temperature in the Parker River estuary at site P22 during 1999 were inversely correlated with discharge from the Parker River into the estuary (Fig. 3a). Salinity remained low through the spring and rose through the summer as discharge dropped. Discharge increased on September 16 after a precipitation event, and salinity remained low subsequently. Note that the 3.5-week loss of data in August to September corresponded to a period of very low discharge (Fig. 3a). Salinity for this period was estimated using the advection–dispersion model developed for this system by Vallino and Hopkinson (1998). Salinity measured on September 6
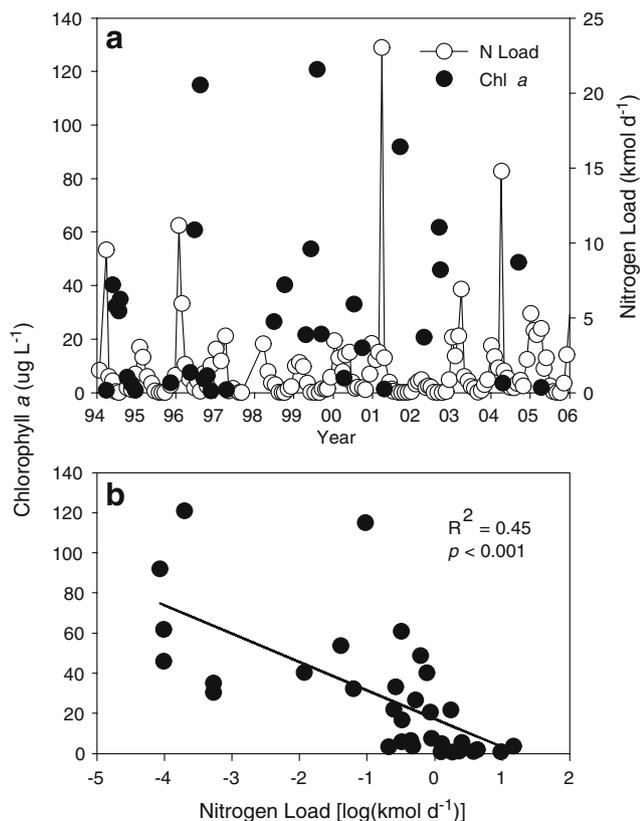
Fig. 2 Time course data (**a**) and relationship between (**b**) dissolved inorganic nitrogen loading from the Parker River to the Parker River Estuary and upper estuarine (within 5 km of the dam) chlorophyll *a* concentration

at low tide at site P22 was 18, which corresponded well with the average daily salinity estimated using the model (Fig. 3a).

Salinity and Nitrogen Pool Surveys

Pore water salinity in the upper sediment layers correlated well with discharge and salinity in the Parker River estuary at sites P24, P22, and P14 and to a lesser degree at P11 and R5.5 (see Fig. 3b for P22 salinity data, other data not shown). Salinities were lower in the spring and late fall when discharge into the system increased. Pore water salinity at sites P24 and P22 ranged from 0 to 17. Fresh water was never found at sites P14, P11, and R5.5, where salinities up to 34 were measured (Table 1). Average salinities at sediment depths >20 cm, where profiles tended to be constant and did not change appreciably over the study period, were 3.8 ($\pm$1.1), 5.6 ($\pm$0.9), 22.1 ($\pm$2.5), 26.7 ($\pm$2.9), and 27.9 ($\pm$2.1) at sites P24, P22, P14, P11, and R5.5, respectively (mean $\pm$ standard deviation).

Pore water and exchangeable NH_4^+ did not exhibit any clear seasonal pattern at any of the sites, and depth profiles were not significantly different on any dates (data not

shown). The seasonally averaged values reflected the down-estuary gradient, with the brackish sites having the highest pore water and exchangeable NH_4^+, while the R5.5 site had the lowest (Fig. 4).

K' values, calculated from the pore water (mM) and exchangeable (μmol cm^{-3}) NH_4^+ adsorption isotherm using all the data from each site (Table 1), indicated that the adsorption capacity of the sediments (on a volumetric basis) decreased from sites P24 to P14. K' was similar at the P14, P11, and R5.5 sites. Note that adsorption isotherm relationships were weak at the P11 and R5.5 sites (Table 1) due in part to lower concentrations of both dissolved and exchangeable NH_4^+ (Fig. 4). When K was calculated, the down-estuary pattern seen for K' was not observed as there were large differences in sediment water content at these sites (Table 1).

While there was no clear seasonal pattern in pore water NH_4^+ or exchangeable NH_4^+ pool sizes at any of the sites, the ratios of pore water to total NH_4^+ at sites P24, P22, and P14 were significantly ($p<0.01$) positively linearly correlated with salinity (Fig. 5). As salinity increased in the pore water, the fraction of total NH_4^+ in the pore water also increased, and the fraction in the exchangeable pool decreased. This effect was greatest at site P22, where the pore water fraction increased by 2.0% with every unit increase in salinity. At salinities near 0, approximately 90% of the total NH_4^+ was adsorbed to sediments at sites P24 and P22. At higher salinities, up to 40% of the total NH_4^+ was dissolved in the pore water at these two sites. This pattern was not evident at the more saline sites P11 and R5.5 (Fig. 5) and, in fact, the relationship appeared to be negative at these sites (significantly so at site P11; $p<0.05$).

The distribution of exchangeable and dissolved NH_4^+ in the sediment exhibited a clear seasonal pattern in relationship to the overlying water salinity at sites P24 and P22 (Fig. 6). The ratio of pore water to total (pore water + exchangeable) NH_4^+ in the top 10 cm was determined for each sampling date. In the spring, when discharge was high and salinity was low, only 10% to 20% of the total NH_4^+ was in the pore water (Fig. 6). As discharge dropped and salinity in the estuary and sediment pore water increased, more of the total NH_4^+ was found in the dissolved fraction at these two sites. The fraction of total NH_4^+ as dissolved NH_4^+ reached a peak in early September, at approximately 28% and 35% dissolved NH_4^+ at sites P24 and P22, respectively (Fig. 6).

Sediment organic carbon content decreased from the freshwater sites to the more saline sites (Table 1). C/N ratios followed a similar gradient (Table 1), with the lowest value at the sandy R5.5 site, approaching the C/N of phytoplankton (6.6, Redfield 1958). There appeared to be a slight increase in the C/N of the sediment from the upper to the midestuary. There was no discernable pattern with depth
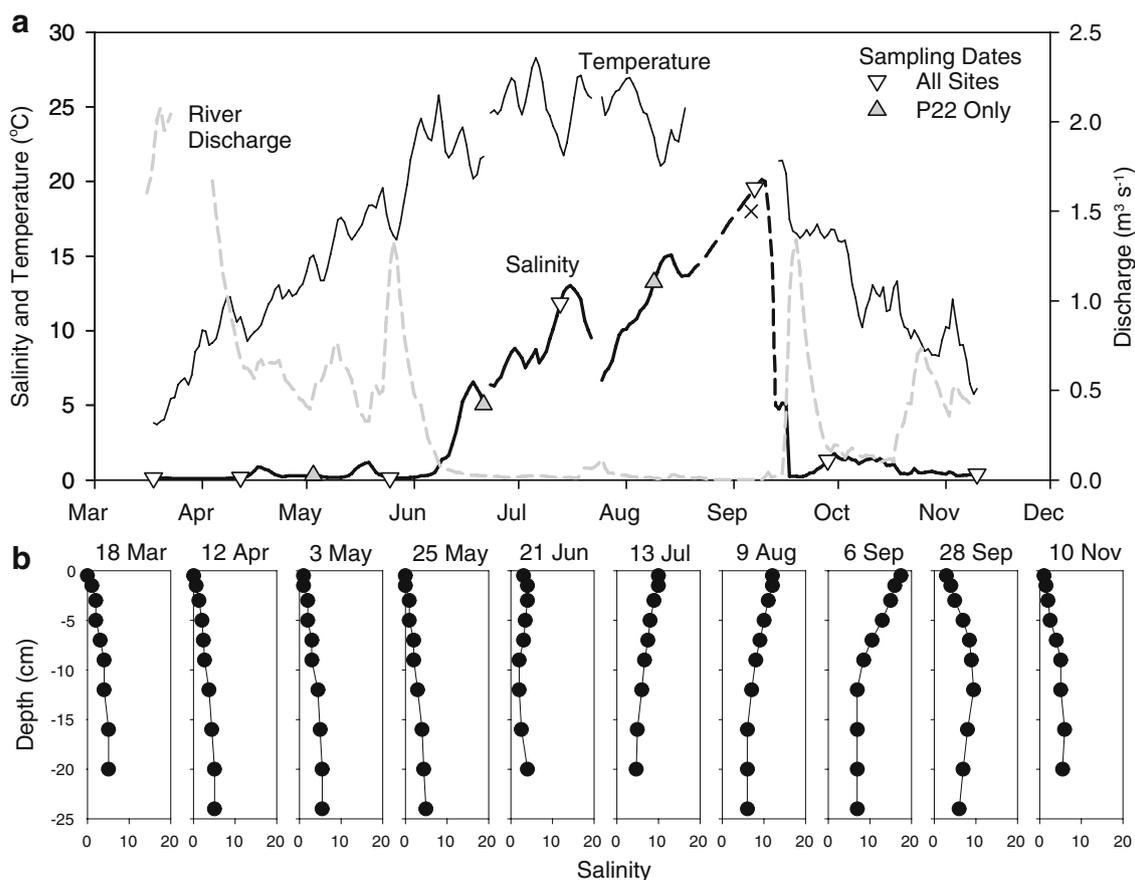
Fig. 3 Average daily discharge from the Parker River and average daily salinity and temperature at site P22 in the Parker River Estuary (**a**) and pore water salinity profiles at site P22 (standard error smaller than points, *n*=2) at ten sampling dates (**b**). Salinity in the estuary is estimated from Aug. 19 through Sep. 13 (*dashed line*, see text), and a low-tide salinity measurement on Sep. 6 is shown (*x mark*). Pore water sampling dates (for all sites and site P22 only) are indicated by *triangles*

at any of the sites except for R5.5 (data not shown), where both the %C and C/N ratios were slightly higher in the surface (0–2 cm) than at depth (10–14 cm).

Laboratory Adsorption Experiment

The laboratory adsorption experiment indicated that salinity greatly affected the exchange capacity of sediment at site P22 (Figs. 7 and 8). When incubated at a salinity of 34, there was little exchangeable NH_4^+ bound to the sediment regardless of dissolved NH_4^+ concentration (Table 2). In contrast, the sediment exposed to freshwater adsorbed 22 μmol $N g^{-1} mM^{-1}$, and a significant portion (approximately 70%) of the total NH_4^+ was bound to sediment exchange sites. The greatest effect on exchange capacity was seen at low salinities, where a shift from a salinity of 0 to 3 reduced the exchangeable pool from 69% to 14%, with relatively little change at the higher salinities (Table 2). Adsorption coefficients calculated from the field data, on a single data point basis, agreed well with laboratory results (Fig. 8).

Pore Water Salinity and Nitrogen Exchange Model

The chloride diffusion model, using only the overlying water salinity and temperature as a function of time and nonenhanced molecular diffusivity, reproduced measured pore water salinity profiles effectively (Fig. 9a). The measured pore water salinities agreed well with modeled values for all dates and depths (slope=0.96; R^2=0.94; $p<0.001$).

The nitrogen exchange model described sediment pore water NH_4^+ profiles that also corresponded quite well with measured profiles (Fig. 9b; slope=1.01; R^2=0.76; $p<0.001$ for all dates and depths). Modeled total and exchangeable NH_4^+ profiles were of similar fit to measured profiles (data not shown). Dissolved NH_4^+ fluxes estimated from the sediment nitrogen exchange model demonstrated a clear effect of the seasonal salinity increase (Fig. 10). In the spring and late fall, the modeled NH_4^+ flux was below 1 mmol m^{-2} day^{-1}, reaching a peak in August of around 4 mmol m^{-2} day^{-1}. The modeled NH_4^+ fluxes showed a similar seasonal pattern as
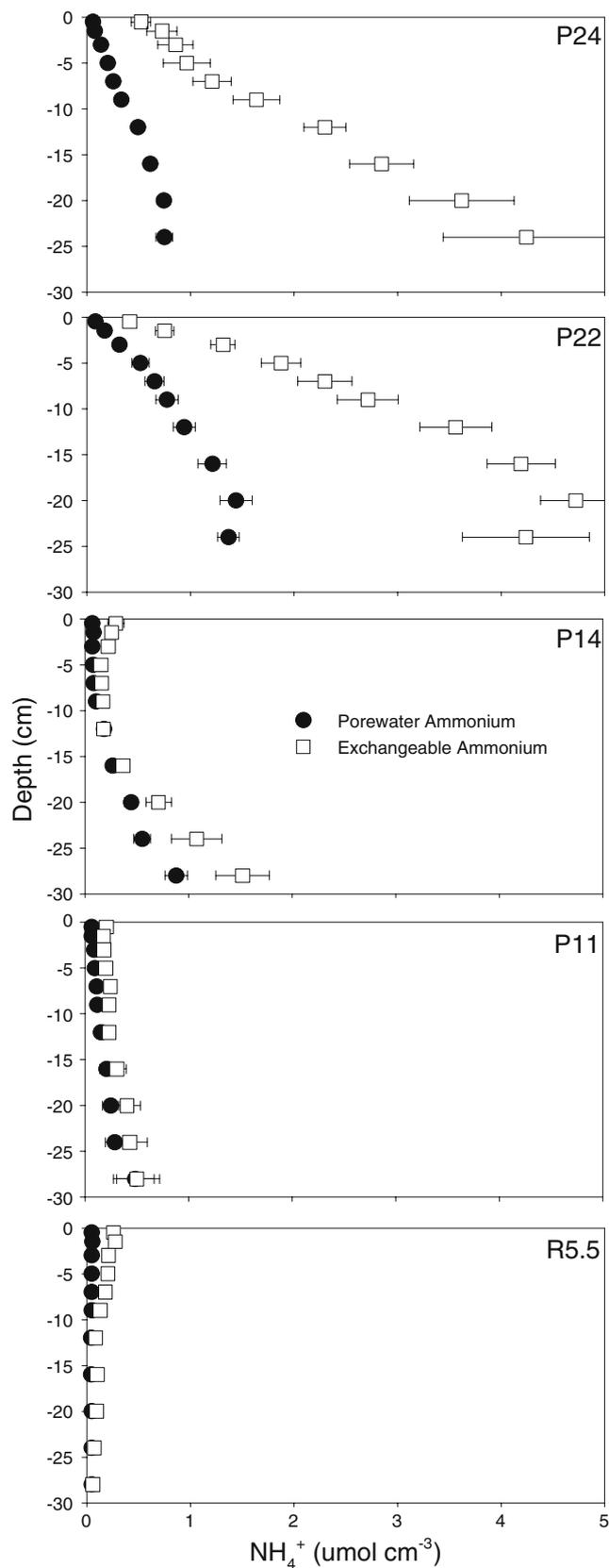
Fig. 4 Sediment depth profiles of average pore water NH_4^+ and exchangeable NH_4^+ (mean ± SE) for seven sampling dates at sites P24, P14, P11, and R5.5 and ten sampling dates at site P22

measured NH_4^+ fluxes from Giblin et al. (2010) for four of the five sampling dates (Fig. 10). Total modeled NH_4^+ flux from the sediments was 537 mmol m^{-2} for the approximately 8-month period.

The nitrogen exchange model was fairly successful in predicting sediment pore water NH_4^+ profiles and flux rates compared with data from the salinity amendment experiment (Fig. 11; Table 3). The model replicated the pore water NH_4^+ maximum at approximately 5-cm depth in the high-salinity treatments, although it somewhat overpredicted NH_4^+ concentrations at depth in the freshwater cores (Fig. 11a). The model underpredicted the effect of changing the salinity from 0 to 8 on the NH_4^+ flux from the sediment to the overlying water during the initial 5 days by 29% (Fig. 11b; Table 3). After the overlying water was changed, the model effectively described the NH_4^+ flux in the salinity treatment (Fig. 11b; Table 3). The model overpredicted the flux in the freshwater in situ treatment by about 30% for the 7-day experiment (Table 3).

The nitrogen exchange model was relatively insensitive to changes in denitrification rates, but the rate of NH_4^+ flux changed markedly if remineralization rates were changed (Fig. 12). Total NH_4^+ flux over the 237 days modeled (537 mmol m^{-2} for base model, scenario A) increased by 4% (22 mmol m^{-2}) if denitrification was halved and decreased by 8% (44 mmol m^{-2}) if denitrification was doubled. Modeled NH_4^+ flux decreased by 29% (156 mmol m^{-2}) when remineralization rates were halved and increased by 58% (311 mmol m^{-2}) when remineralization was doubled (Fig. 12). This is consistent with the observation that denitrification rates are low (0.2–1.0 mmol m^{-2}day^{-1}) relative to estimated mineralization rates (1–6 mmol m^{-2}day^{-1}) at this site (Giblin et al. 2010).

The depth distribution of the net NH_4^+ production, R, was not directly measured in our experiments. Sensitivity analysis of the nitrogen exchange model demonstrated that the model was fairly sensitive to changes in the distribution of R (Fig. 13). Higher overall NH_4^+ flux was predicted when R was relatively higher in the shallow sediment (i.e., scenarios F and G), and lower overall NH_4^+ flux when R was more evenly distributed with depth (scenario H). Total NH_4^+ flux was 31% (164 mmol m^{-2}) and 21% (112 mmol m^{-2}) higher in scenarios F and G, respectively, than in the base model scenario A. Scenario H, with relatively more NH_4^+ production at depth (Fig. 13), had 30% (163 mmol m^{-2}) less total NH_4^+ flux than the base model. A significant buildup of total NH_4^+ occurred at depth in scenario H (about 1 μmol cm^{-3}), suggesting that this may not be a reasonable R distribution (Fig. 13). A k of 0.2 (scenario A), as the more conservative estimate of NH_4^+ flux, was the equation used in our final model (Figs. 9 and 10).
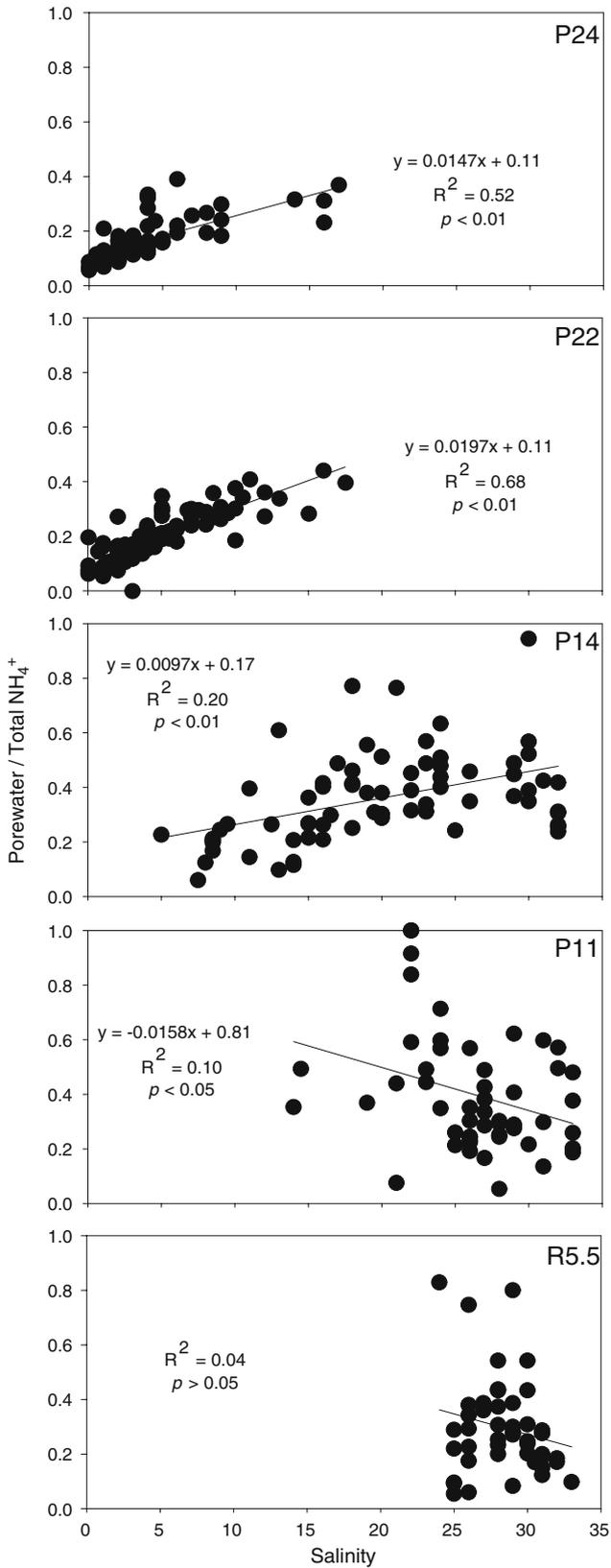
Fig. 5 Pore water to total NH_4^+ ratios versus pore water salinity at five sites in the Parker River Estuary
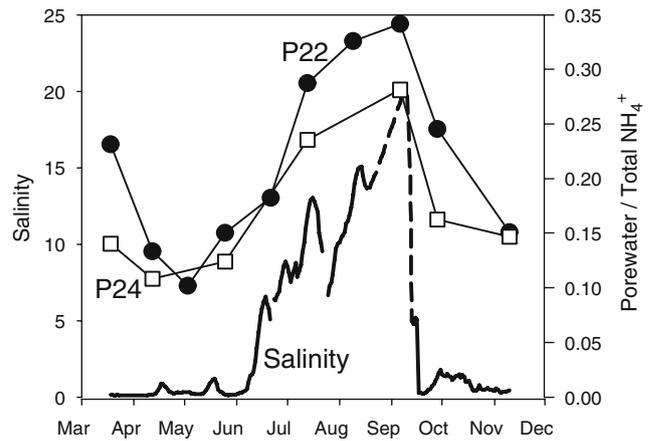

Fig. 6 Pore water to total NH_4^+ ratios (of profiles integrated to a depth of 10 cm) at sites P24 and P22 over the sampling period, with salinity shown at site P22 for reference

While the overall magnitude of the NH_4^+ flux was sensitive to changes in remineralization rate and distribution, the effect of seasonal changes in salinity on the NH_4^+ flux was similar across model runs (Figs. 12 and 13). The increase in NH_4^+ flux from the first of June (before salinity had a major effect) to the peak flux in the middle of July (when salinity was highest) doubled regardless of denitrification or remineralization rate (scenarios A–E; Fig. 12) and increased by 66%, 82%, and 121% in scenarios F, G, and H, respectively.

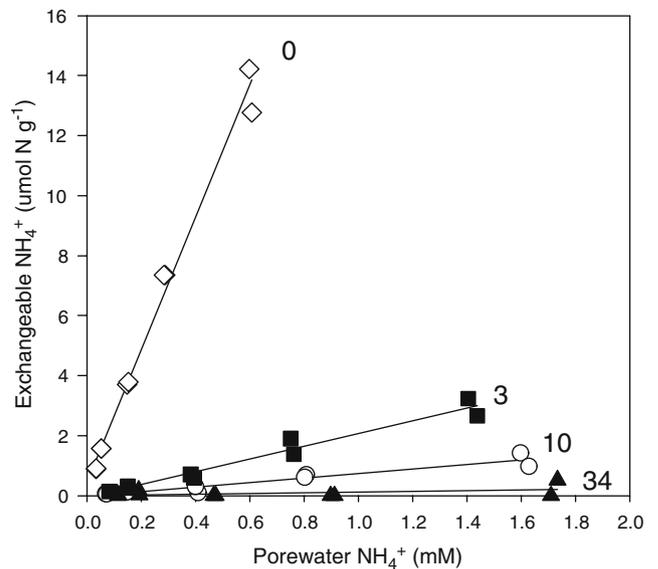The nitrogen exchange model predicted significant changes in the timing and magnitude of sediment NH_4^+ flux

Fig. 7 Pore water and exchangeable NH_4^+ concentrations at four salinities in laboratory-manipulated sediment from site P22. Adsorption coefficients are given in Table 2
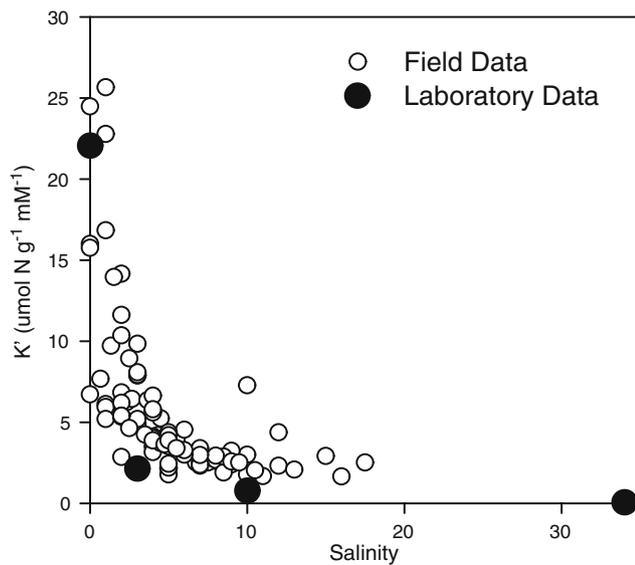
Fig. 8 K' values from laboratory-manipulated sediment and from individual field measurements at site P22 at varying salinities

in years with different seasonal salinity regimes (Fig. 14). Compared to the normal year, total NH_4^+ flux for the 5-month period (May–Sep) was 11.5% higher in the dry year and 18% lower in the wet year. The timing of the maximum flux was also shifted earlier in the summer in the dry year compared with the normal water year. For the 5-month summer period, the average flux was 0.84 mmol $m^{-2}day^{-1}$ higher in the dry year than in the wet year.

Twice daily tidal salinity oscillations of up to 12 were measured for much of June, July, and August at site P22 (Fig. 15). When these tidal salinity oscillations were incorporated into the nitrogen exchange model, the model predicted tidal oscillations in the NH_4^+ flux of up to 1.5 mmol $m^{-2}day^{-1}$, and oscillations of 1.0 mmol $m^{-2}day^{-1}$ were common for much of June, July, and August (a 2-week period in August is shown in Fig. 15). Incorporation of tidal salinity into the model did not significantly change the overall magnitude of NH_4^+ flux from the sediments, however, as there was less than 1% difference between the total seasonal flux from the average daily and half-hour salinity models (537 and 542 mmol m^{-2}, respectively).

Discussion

Nitrogen Stocks

Patterns of pore water and exchangeable NH_4^+ in sediments (Fig. 4) and pore water salinities (Fig. 3 for site P22, other data not shown) of the five sampling sites illustrate a down-estuary gradient of sediment type and nitrogen pools. Sites

P24 and P22 have relatively high pore water and exchangeable NH_4^+ that increase with depth and salinity in the surface sediments that reflected recent overlying water salinity, converging to an annual average at approximately 25 cm. These two sites were organic-rich (Table 1), diffusion-driven, muddy sediments with little or no bioturbation. Sites P14, P11, and R5.5 had lower levels of pore water and exchangeable NH_4^+ (Fig. 4), often constant with depth or exhibiting non-steady-state profiles. Pore water salinity at P11 and R5.5 often mirrored overlying water salinity for the depth of the core and to a depth of 10 cm at site P14 (data not shown). These three sites, with coarse mud to sandy sediments and lower organic content (Table 1), may be periodically or regularly flushed. Bioirrigation also plays a role in altering the pore water profiles, as *Mya arenaria* (soft-shelled clam) was found in high densities at site P14.

Pore water and exchangeable NH_4^+ exhibited no clear temporal pattern at any of the five sites. This was expected at sites P14, P11, and R5.5, where flushing and bioturbation controlled the profiles of NH_4^+. At sites P24 and P22, the lack of temporal differences was most likely due to slight differences in sampling locations between dates and difficulty in identifying relatively small seasonal changes in NH_4^+ with large background concentrations. There was, in contrast, a clear temporal pattern in the pore water to exchangeable NH_4^+ ratio at sites P24 and P22 (Fig. 6). Additionally, a clear positive relationship was observed between the pore water to exchangeable NH_4^+ ratio and pore water salinity at sites P24, P22, and P14 (Fig. 5).

Ammonium Adsorption

In sediments of the upper and mid Parker River estuary (P24, P22, and P14), the dissolved fraction of NH_4^+ was highly influenced by pore water salinity (Figs. 5, 6, 7, and 8, Table 2). Dissolved pore water NH_4^+ can range from about 10% to 40% of the total NH_4^+ at sites P24 and P22, depending on pore water salinity (Fig. 5). As these sites have substantial stocks of NH_4^+ (Fig. 4), pore water NH_4^+ concentrations at these stations can exceed 3 mM.

Table 2 K', K, and the fraction of exchangeable NH_4^+ to total NH_4^+ for salinity-manipulated sediments from site P22

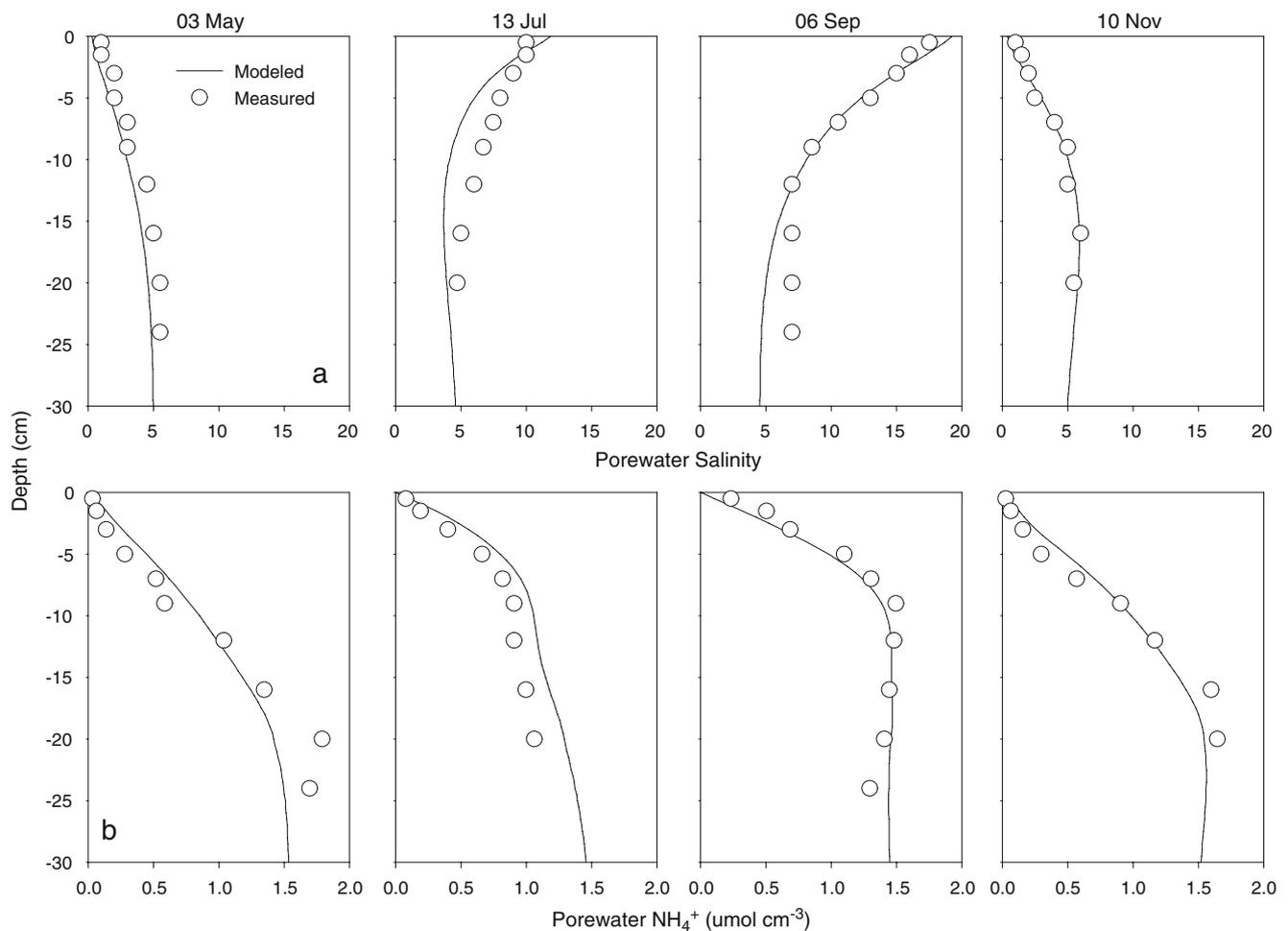| Salinity	K' (μmol N g^{-1} mM^{-1})	K	Exchangeable NH_4^+ (fraction of total NH_4^+)
0	22.07	19.12	0.689
3	2.11	1.83	0.136
10	0.76	0.66	0.059
34	0.04	0.03	0.007

Fig. 9 Examples of model output for pore water salinity (a) and pore water NH_4^+ (b) for four dates compared with measured salinity and pore water NH_4^+ at site P22

Our results are comparable to other studies of dissolved and exchangeable NH_4^+ in freshwater and saline sediments. In a review of the literature, Seitzinger et al. (1991) found that freshwater sediments typically had higher exchangeable to dissolved NH_4^+ (K') values, ranging from approx-imately 2 to 65 μmol $Ng^{-1}mM^{-1}$, while in marine sediments the ratio reached a maximum of about 18 μmol $Ng^{-1}mM^{-1}$. Our laboratory adsorption experiment found a decrease in K' from 22 to 0.04 μmol $Ng^{-1}mM^{-1}$ when sediments from site P22 were switched from fresh to

Fig. 10 Model output of NH_4^+ flux from the sediment at site P22, with salinity and net NH_4^+ production (R) shown for reference. Measured NH_4^+ fluxes ($\pm$ SE) from site P22 (Giblin et al. 2010) are shown for comparison
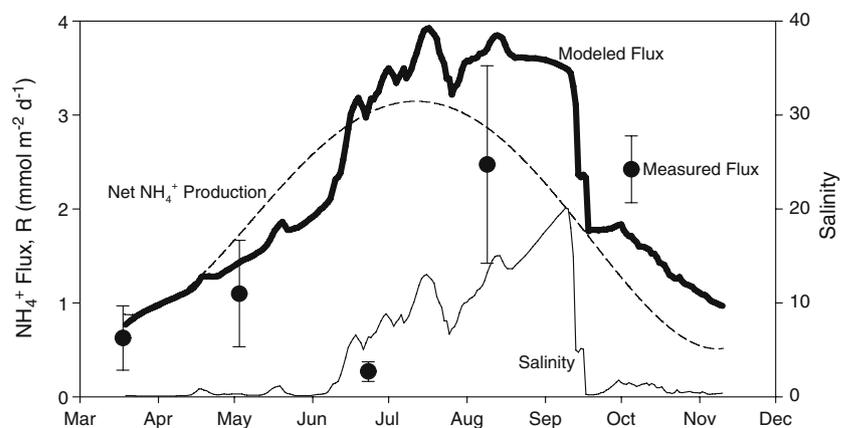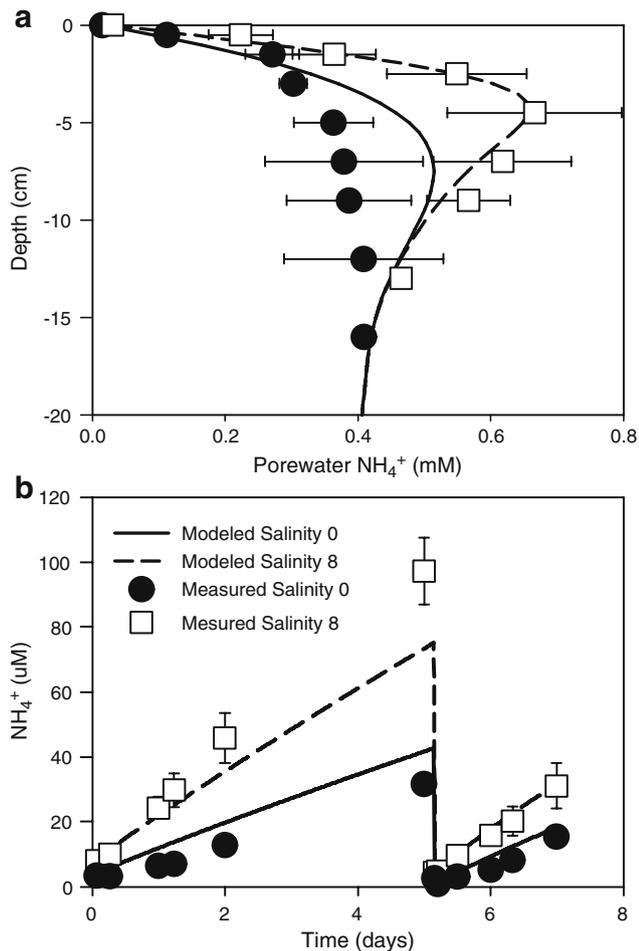
Fig. 11 Measured experimental results (mean ± SE, *n*=2) and model results of pore water NH_4^+ profiles at the termination of the experiment (**a**) and time course overlying water NH_4^+ concentration (**b**) from site P22 sediment core incubations with freshwater and salinity-amended (salinity of 8) overlying water. *Symbols* in the *lower panel* apply to both panels. The measured and modeled NH_4^+ flux rates from the initial 5 days and the final 2 days (after the water overlying the core was changed) are given in Table 3

a salinity of 34 (Figs. 7 and 8, Table 2). Hou et al. (2003) measured a similar effect of salinity on the adsorption of NH_4^+ in sediments from the Yangtze Estuary, although the effects of salinity were not as pronounced in those sediments.

The low *K′* and *K* values of P22 sediment at higher salinities (Table 2) suggest that these sediments have a relatively low absolute exchange capacity. These values are in contrast to a *K* value of 1.3±0.1 found for a wide range of marine sediments (Mackin and Aller 1984). Although a *K* value of 19.1 was measured when sediments from P22 were fresh, the *K* value dropped to 0.03 when exposed to seawater. This may be due to lack of negatively charged clay minerals or organic matter in P22 sediments from this site (Rosenfeld 1979).

Sites P11 and R5.5, where salinity was consistently above 10 (Table 1), do not appear to be affected by salinity (Fig. 5). Stocks of inorganic nitrogen were lower at these sites (Fig. 4), and NH_4^+ flux measured at the R5.5 site by Hopkinson et al. (1999) were always low (<0.5 mmol m^{-2} day^{-1}). Therefore, the salinity desorption effect had the greatest impact on the upper and midestuary sites. Higher stocks of nitrogen and larger seasonal changes in salinity at sites P24, P22, and to a lesser extent at P14 indicate that nitrogen cycling was significantly influenced by salinity in the upper Parker River estuary.

Salinity and Ammonium Flux: Insights from the Model

The chloride diffusion and nitrogen exchange models were quite successful in predicting sediment chloride and NH_4^+ profiles at site P22 over the course of the approximately 8-month study (Fig. 9). This relatively simple model employed only nonenhanced molecular diffusion for the flux of Cl^- and NH_4^+, and the modeled chloride distributions were used as a driver in determining the pore water NH_4^+ component of the nitrogen exchange model based on the measured relationship of pore water to total NH_4^+ at site P22 (Figs. 5, 6, 7, and 8). All model parameters were held constant during a model run, with the exception of the overlying water salinity, temperature (used to calculate the diffusion coefficient), and net NH_4^+ produced from organic matter mineralization (*R*). The model parameters are either measured directly (salinity, temperature, adsorption, porosity, denitrification rates) or are well defined in the literature (diffusion coefficients), with the exception of the rate of *R*. The modeled NH_4^+ flux is sensitive to NH_4^+ production rates (Fig. 12) and to the depth distribution of the NH_4^+ production (Fig. 13), but both parameters are relatively poorly constrained. NH_4^+ production rates and depth distributions are therefore the most likely sources of error to the model.

Table 3 Measured and modeled ammonium flux rates (mmol m^{-2} day^{-1}) from site P22 sediments with freshwater and salinity-amended (salinity of 8) overlying water in the initial 5 days and the final 2 days after water overlying each core was changed (see Fig. 11)

Salinity	NH_4^+ flux (mmol m^{-2} day^{-1})	
	Measured	Modeled
Initial flux rates		
0	1.6	2.0
8	4.8	3.4
Final flux rates		
0	1.9	2.5
8	3.7	3.9

Fig. 12 Sensitivity of the modeled NH_4^+ flux rates to the halving or doubling of denitrification (scenarios *B* and *C*, respectively) and remineralization (scenarios *D* and *E*, respectively) rates from base model rates (scenario *A*)
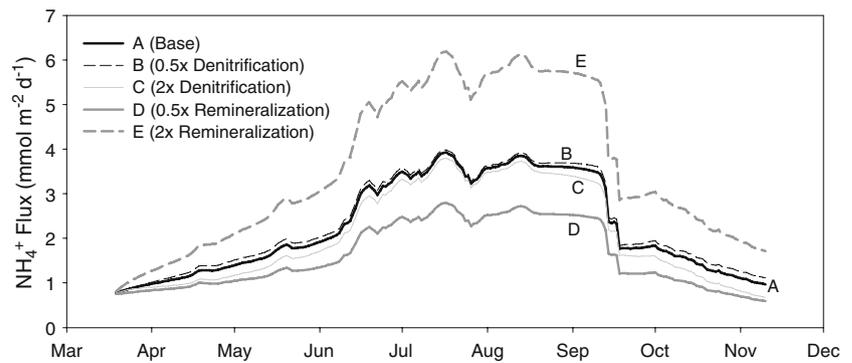
NH_4^+ production in the model was estimated from benthic metabolism (using DIC flux rates measured five times during this study, see Giblin et al. 2010) and a C/N ratio (12.7) of the organic matter mineralized (Fig. 10). The C/N ratio of organic matter undergoing remineralization in aquatic sediments can vary widely, from apparently nitrogen-rich organic matter with C/N below the Redfield (1958) ratio of 6.6 (Zimmerman and Benner 1994; Aller et al. 2004; Weston et al. 2006) to nitrogen-poor organic matter with C/N ratios exceeding 30 (Eyre and Ferguson 2005). The C/N ratio of the bulk sediment (15; Table 1) is unlikely to reflect the composition of the mineralized organic matter due to preferential mineralization of nitrogen relative to the bulk sediment organic matter (Burdige 1991; Zimmerman and Benner 1994; Kristensen and Hansen 1999). Contributions of nitrogen-rich organic matter from

Fig. 13 Sensitivity analyses of the nitrogen exchange model to changes of the depth distribution of net NH_4^+ production (*R*) in the sediment. *R* is defined by the equation $R = \alpha e^{-kz}$, and *k* is varied from the base model value of 0.2 (scenario *A*) to 1.0, 0.5, and 0.05 (scenarios *F*, *G*, and *H*, respectively). The cumulative fraction of R with depth (**a**) described by these varying *k* values and the resulting total NH_4^+ profiles at the end of the approximately 8-month model runs (**b**) and time course NH_4^+ flux rates (**c**) are shown
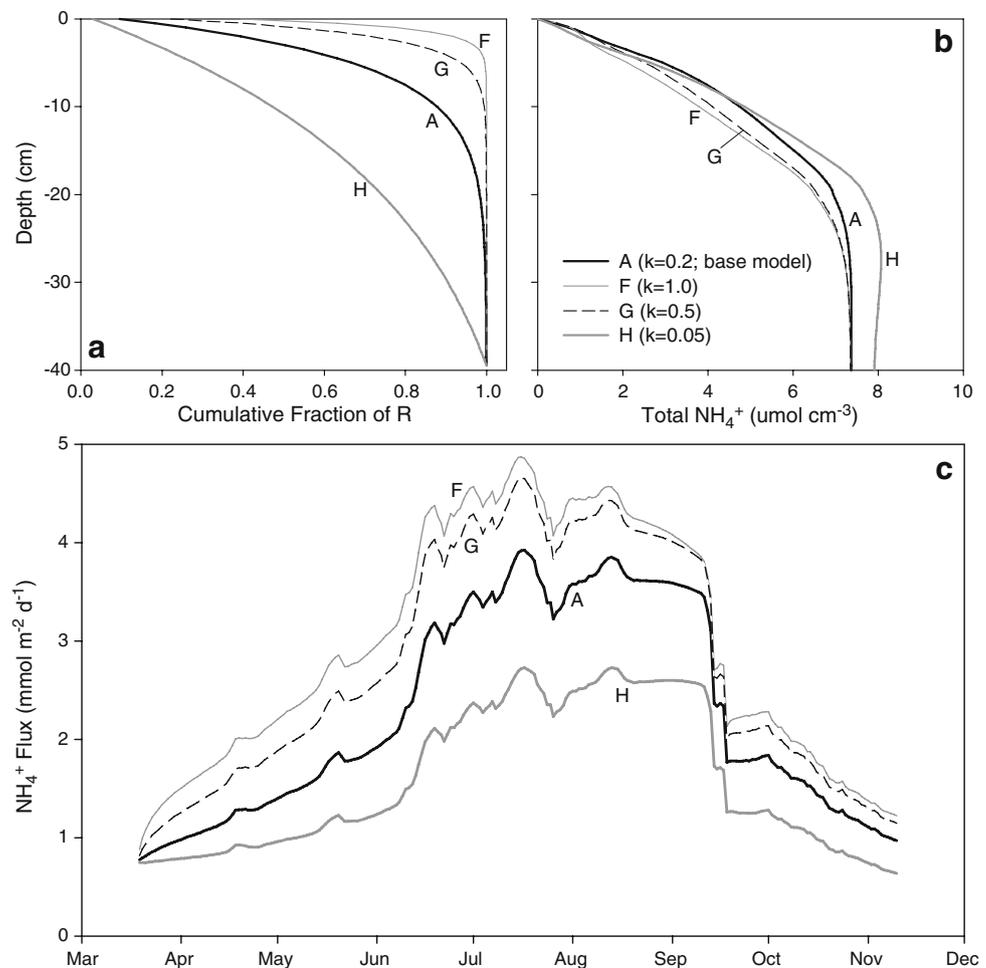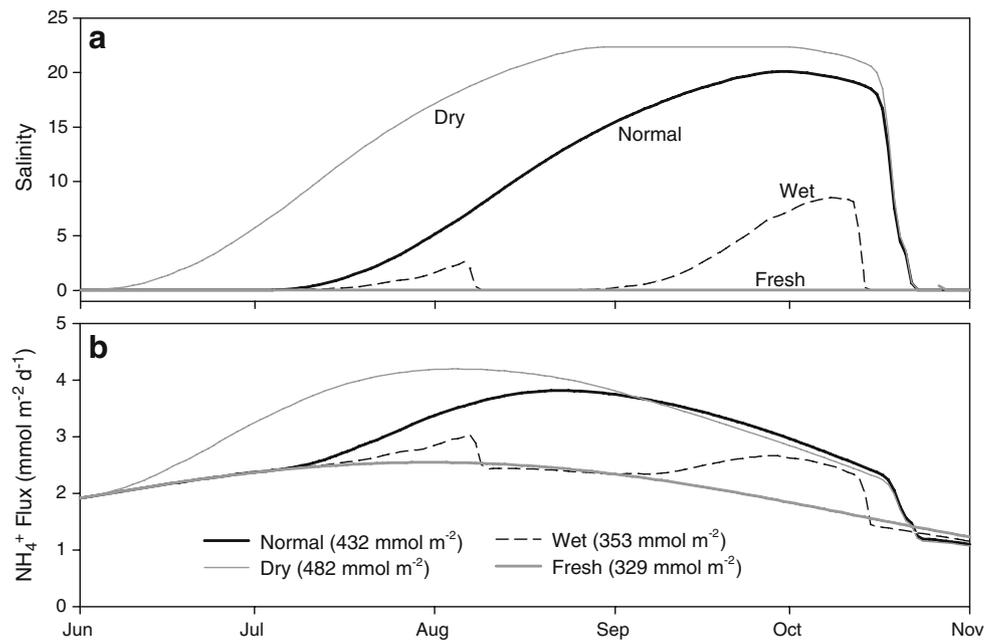
Fig. 14 Results from four nitrogen exchange model runs using the same parameters, varying only the seasonal salinities to simulate normal, dry, wet, and freshwater years and the resulting salinity in the estuary (**a**) and the NH_4^+ flux (**b**). The total flux of NH_4^+ from the sediments for the 5-month period is indicated for each scenario


phytoplankton, bacterial biomass, or anthropogenic inputs (Grill and Richards 1964; Zimmerman and Benner 1994; Weston et al. 2006), as well as delivery of terrestrially derived organic matter with higher C/N ratios (Thornton and McManus 1994), can result in changes in the C/N ratio of decomposing organic matter.

Deviations in the C/N of the mineralized organic matter from the value used in the nitrogen exchange model would alter the NH_4^+ production rate and thus the modeled NH_4^+ flux. A doubling of the NH_4^+ remineralization rate

(scenario E, Fig. 12) is the equivalent of halving the C/N ratio, which then approaches the Redfield (1958) ratio of 6.6. Similarly, halving the NH_4^+ remineralization rate (scenario D; Fig. 12) demonstrates the model's sensitivity to either lower overall NH_4^+ mineralization rates or an increase in the C/N to ~25. Not surprisingly, the overall NH_4^+ flux rates were higher when NH_4^+ mineralization rates were greater (scenario D; Fig. 12), and flux rates were lower when NH_4^+ mineralization rates were lower (scenario E; Fig. 12). Modeled NH_4^+ flux from the sediment is

Fig. 15 Incorporation of tidal salinity oscillations (using 0.5-h measurements of salinity) compared with average daily salinities (**a**) on the nitrogen exchange model predicted NH_4^+ flux (**b**). A 2-week period in August is shown to demonstrate the tidal oscillations
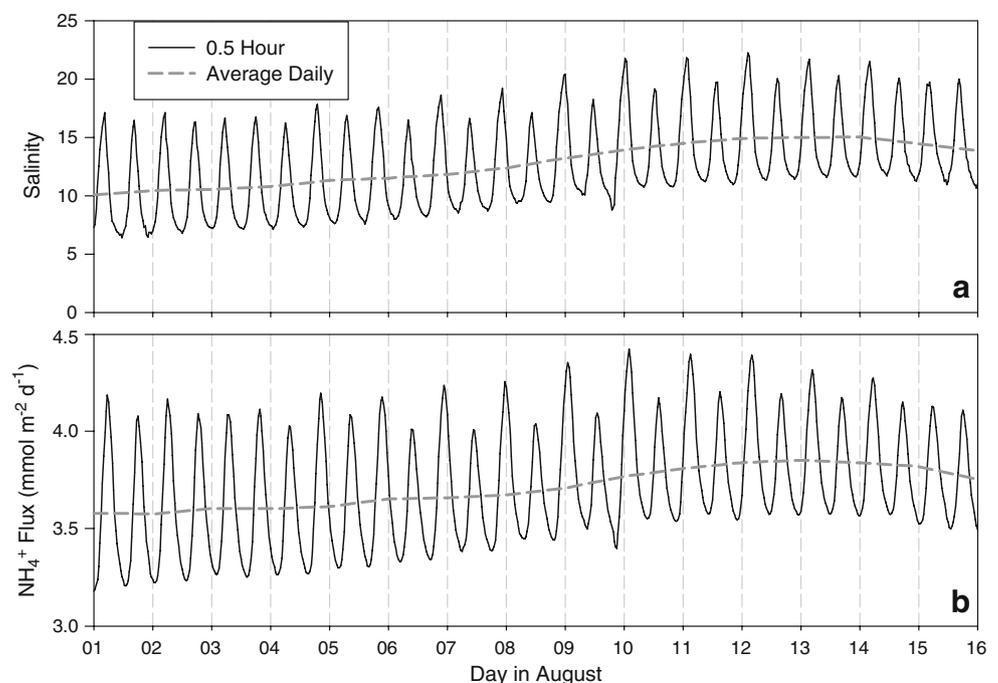
clearly sensitive to the rate of NH_4^+ production and therefore also to the C/N ratio used in the model.

The model also demonstrated sensitivity to the depth distribution of NH_4^+ production (Fig. 13). Organic matter mineralization is likely higher near the sediment–water interface where organic matter delivery is highest, although substantial variability in mineralization rates with depth has been observed (i.e., Aller et al. 2004). The nitrogen exchange model suggests that NH_4^+ flux rates were highest when a greater proportion of total NH_4^+ production occurred near the sediment–water interface (scenarios F and G; Fig. 13). Conversely, as NH_4^+ production rates were more evenly distributed with sediment depth, predicted NH_4^+ flux rates were lower (scenario H; Fig. 13). The accumulation of NH_4^+ at depth in scenario H (Fig. 13) suggests that this scenario is not a reasonable estimate of the depth distribution of organic matter mineralization, which confirms the assumption of more steeply declining rates with depth.

The model does not account for many aspects of the seasonal dynamics of nitrogen cycling in estuarine sediments such as a shifts in the depth distribution of NH_4^+ production or in the C/N ratio of the organic matter over time. For instance, as river discharge declines and estuarine water column productivity increases during the summer (Fig. 2), delivery of organic matter to the sediments is likely to shift from predominantly marsh and terrestrially-derived to phytoplankton in origin, with a concomitant decline in C/N ratios. Freshly deposited organic material on the sediment surface, such as would occur following a spring bloom, would likely alter the depth distribution of NH_4^+ production. The coupling of the nitrogen exchange model with more extensive data on estuarine production and delivery of organic material to the sediment would likely yield a better estimate of organic matter mineralization and patterns of NH_4^+ flux from the sediments.

Despite the uncertainties associated with NH_4^+ production in the nitrogen exchange model, the model was remarkably successful at predicting NH_4^+ flux from experimental salinity-amended sediment cores (Fig. 11, Table 3), and the sensitivity analyses all demonstrated that increasing salinity enhanced desorption and subsequent diffusion of NH_4^+ from these sediments (Figs. 12 and 13). From 1 June (just before the summer salinity increase at site P22; Fig. 3) to peak NH_4^+ flux in mid-July, modeled NH_4^+ flux doubled regardless of remineralization and denitrification rate (scenarios A–E; Fig. 12), and modeled NH_4^+ flux increased by 66%, 82%, and 121% over the same period in scenarios F, G, and H, respectively. These results suggest that the depth distribution of NH_4^+ production may have the greatest influence on the relative impact of salinity on NH_4^+ flux rates. We believe the model clearly demonstrates

the effects of salinity on benthic fluxes of NH_4^+ from these estuarine sediments both quantitatively and qualitatively.

The model predicted NH_4^+ fluxes that compared relatively well for four of the five dates on which measurements were made (Fig. 10) and was successful in describing the flux NH_4^+ from sediments at site P22 in a salinity amendment experiment (Fig. 11, Table 3). A low flux measured by Giblin et al. (2010) in June (Fig. 10) was not predicted by either our model or our understanding of the biogeochemical processes in these sediments (the DIC flux on this date exceeded the rates in March, May, and October, Giblin et al. 2010). Dark uptake by benthic microalgae (Anderson et al. 2003) or sediment bacteria (Rivera-Monroy and Twilley 1996; Eyre and Ferguson 2005) may be responsible for immobilization of some portion of the mineralized NH_4^+ in the early spring in these sediments. NO_x fluxes were directed out of the sediment on this date (Giblin et al. 2010), indicating that rates of nitrification may have been unusually high at this time. However, rates of NO_x flux were small (0.1 mmol m^{-2} day^{-1}), and nitrification and subsequent efflux of NO_x do not account for the "missing" NH_4^+.

Salinity-mediated ammonium flux may be an important process in estuarine sediments where salinities can change on daily (tidal), seasonal, and yearly timescales. The pattern of higher salinities in the upper reaches of the estuary during the summer when freshwater discharge from the watershed is low results in a seasonal pattern of increased desorption-driven NH_4^+ flux from the sediments in the summer (Fig. 10) as suggested by Hopkinson et al. (1999). However, this seasonal pattern may vary substantially from year to year, depending on the amount and timing of precipitation in the watershed.

Due to the length of the Parker River (~14 km from the dam to Plum Island Sound, Fig. 1), even small increases in freshwater river discharge can influence the salinity in the upper estuary. In mid-July, for example, an increase in river discharge to only approximately 0.1 m^{3}s^{-1} reduced salinities at site P22 from 13 to 7 (Fig. 3). Furthermore, in the largely advection-dominated upper reaches of the estuary, the long water residence times during periods of low discharge (Vallino and Hopkinson 1998) result in slow increases in salinity. It takes several weeks of very low discharge to reach salinities above 10 (Fig. 3). Yearly differences in watershed precipitation, especially even small differences in the summer months, may significantly alter the pattern of salinity-driven flux of NH_4^+ from the sediments in the upper estuary.

Nitrogen exchange model simulations of four different hypothetical water years demonstrated that changes in the pattern of discharge and the resulting salinity regime in the Parker River can significantly alter the timing and magnitude of the flux of NH_4^+ from the sediments in the upper

estuary. In dry years with less spring discharge and earlier salinity increases, the overall magnitude of the NH_4^+ flux is greater and the peak flux is shifted earlier in the summer (Fig. 14). Conversely, in wet years, the overall sediment NH_4^+ flux is lower, and a midsummer precipitation event can markedly decrease the supply of NH_4^+ to the overlying water. Such changes can have important consequences for the timing of phytoplankton blooms, as discussed below.

The model also suggested that tidal salinity oscillations in the upper estuary, where daily fluctuations in salinity of 10 or more during periods of low discharge were observed, can result in oscillations of 1.0 mmol m^{-2} day^{-1} or more in the NH_4^+ flux (Fig. 15). Caetano et al. (1997) measured NH_4^+ flux from intertidal sediments during a flooding tide and confirmed a loss of adsorbed NH_4^+ from the surficial sediment. Concentrations of NH_4^+ in estuarine waters are often higher on the ebb tide than on the flood tide, which is usually attributed to a benthic or marsh source of NH_4^+ (i.e., Yin and Harrison 2000; Magni et al. 2002). Tidal oscillations in salinity and NH_4^+ release from the sediments, resulting in peak NH_4^+ flux at high tide, may in part also contribute to these observations in some systems.

Importance to Estuarine Productivity

As freshwater flow into the Parker River estuary declines in the late spring, inorganic nitrogen inputs drop to insignificant levels, but estuarine chlorophyll *a* concentrations often increase in the upper reaches (Fig. 2). When river discharge is high (greater than ~0.5 m^3 s^{-1}), the hydrologic residence time of the upper estuary is too short to support a bloom (Wright et al. 1987; Vallino and Hopkinson 1998) and phytoplankton are flushed out of the system. When river discharge drops and the hydrology becomes favorable for a bloom, the nitrogen loading from the Parker River drops to insignificant levels. Holmes et al. (2000) found that riverine inputs of inorganic nitrogen could account for only about 10% of primary production in the upper Parker River estuary during the late summer. While groundwater and atmospheric inputs of nitrogen and rapid recycling of nitrogen in the water column may help fuel the phytoplankton, these sources are most likely small compared to benthic NH_4^+ release in the upper Parker River estuary (Holmes et al. 2000).

Total system gross primary production was estimated by Balsis et al. (1995) at 2.1 gC m^{-2} day^{-1} for the upper Parker River estuary. More recent calculations of low-discharge summer total system gross primary production in the upper estuary over a number of years average 2.4 gC m^{-2} day^{-1} (Hopkinson and Weston, *unpublished data*). Assuming a primary production stoichiometric C/N demand ratio of 106:16 (Redfield 1958), N demand in the upper estuary was estimated at 26–30 mmol N m^{-2} day^{-1}. Direct measurement of benthic metabolism and nutrient flux in the upper Parker River estuary yielded estimates of 30–40% of the N demand for primary producers met by the sediments (Hopkinson et al. 1999).

Model estimates from the current study indicate that salinity-mediated desorption can approximately double NH_4^+ fluxes from the sediments for a limited period of time (weeks to months; Fig. 14). When remineralization is 2.5 mmol m^{-2} day^{-1}, there is a salinity-driven increase from 2.3 to 4.0 mmol N m^{-2} day^{-1} (at a salinities of 0 and 20, respectively), increasing the relative importance of benthic NH_4^+ release in supporting estuarine primary production. We expect that desorption and flux of NH_4^+ from the sediments is evident at seasonal, lunar, and daily timescales, as discharge, spring–neap tides, and daily high–low tides, respectively, influence salinity in the estuary. For example, daily salinity oscillations of over 12 were measured at site P22, which was estimated by the nitrogen exchange model to cause a ~1 mmol m^{-2} day^{-1} oscillation in NH_4^+ flux from the sediment (Fig. 15).

We believe our data and the model demonstrate that salinity-mediated desorption and flux of NH_4^+ from the sediments of the upper Parker River estuary is a potentially important source of inorganic nitrogen to primary producers when inputs from the watershed are low. This process can, for limited periods of time, be as significant a source of N to the water column as benthic remineralization.

Application to Other Estuaries

The processes of salinity-mediated desorption and subsequent flux of NH_4^+ from the sediments of the Parker River estuary as described here may be important in other coastal systems. The only requisite is that salinities change significantly enough to influence the equilibrium between pore water and exchangeable NH_4^+. This process is likely to have the greatest impact on sediments that change from predominately fresh to brackish seasonally. Indeed, this process may lead to more pronounced salinity-mediated NH_4^+ flux in other estuarine systems, as only about 20% of total system respiration in the Parker River takes place in the benthos, which is lower than most other shallow estuaries (Hopkinson et al. 1999; Boynton and Kemp 1985). Furthermore, the NH_4^+ adsorption capacity of sediments in the Parker River (Table 2) is fairly limited compared to other estuarine sediments (Seitzinger et al. 1991). Sediments from other systems may therefore contain more total NH_4^+ (due to higher rates of benthic remineralization), have the capacity to adsorb more NH_4^+, and

potentially have enhanced fluxes of NH_4^+ from sediments due to salinity increases.

References

Aller, R.C., C. Heilbrun, C. Panzeca, Z. Zhu, and F. Baltzer. 2004. Coupling between sedimentary dynamics, early diagenetic processes, and biogeochemical cycling in the Amazon–Guianas mobile mud belt: coastal French Guiana. *Marine Geology* 208: 331–360.

Anderson, I.C., K.J. McGlathery, and A.C. Tyler. 2003. Microbial mediation of 'reactive' nitrogen transformations in a temperate lagoon. *Marine Ecology Progress Series* 246: 73–84.

Balsis, B.R., D.W.M. Alderman, I.D. Buffam, R.H. Garritt, C.S. Hopkinson Jr., and J.J. Vallino. 1995. Total system metabolism of the Plum Island Sound estuarine system. *Biological Bulletin* 189: 252–254.

Berner, R.A. 1980. *Early diagenesis, a theoretical approach*. Princeton: Princeton University Press.

Boatman, C.D., and J.W. Murray. 1982. Modeling exchangeable NH4+ adsorption in marine sediments: Process and controls of adsorption. *Limnology and Oceanography* 27: 99–110.

Boudreau, B.P. 1997. *Diagenetic models and their implementation*. Berlin: Springer.

Boynton, W.R., and W.M. Kemp. 1985. Nutrient regeneration and oxygen consumption by sediments along an estuarine salinity gradient. *Marine Ecology Progress Series* 23: 45–55.

Burdige, D.J. 1991. The kinetics of organic matter mineralization in anoxic marine sediments. *Journal of Marine Research* 49: 727–761.

Caetano, M., M. Falcão, C. Vale, and M.J. Bebianno. 1997. Tidal flushing of ammonium, iron and manganese from inter-tidal sediment pore waters. *Marine Chemistry* 58: 203–211.

Eyre, B.D., and A.J.P. Ferguson. 2005. Benthic metabolism and nitrogen cycling in a subtropical east Australian estuary (Brunswick): Temporal variability and controlling factors. *Limnology and Oceanography* 50: 81–96.

Finstein, M.S., and M.R. Bitzky. 1972. Relationships of autotrophic ammonium-oxidizing bacteria to marine salts. *Water Research* 6: 31–40.

Gardner, W.S., S.P. Seitzinger, and J.M. Malczyk. 1991. The effects of sea salts on the forms of nitrogen released from estuarine and freshwater sediments: Does ion pairing affect ammonium flux? *Estuaries* 14: 157–166.

Giblin, A.E., C.S. Hopkinson Jr., and J. Tucker. 1997. Benthic metabolism and nutrient cycling in Boston Harbor, Massachusetts. *Estuaries* 20: 346–364.

Giblin, A.E., N.B. Weston. G.T. Banta, J. Tucker and C.S. Hopkinson Jr. 2010. The effects of salinity on nitrogen losses from an oligohaline estuarine sediment. *Estuaries and Coasts*. doi:10.1007/s12237-010-9280-7.

Grill, E.V., and F.A. Richards. 1964. Nutrient regeneration from phytoplankton decomposing in sea water. *Journal of Marine Research* 22: 51–69.

Hartnett, H.E., and S.P. Seitzinger. 2003. High-resolution nitrogen gas profiles in sediment pore water using an new membrane probe for membrane-inlet mass spectrometry. *Marine Chemistry* 83: 23–30.

Holmes, R.M., B.J. Petersen, L.A. Deegan, J.E. Hughes, and B. Fry. 2000. Nitrogen biogeochemistry in the oligohaline zone of a New England estuary. *Ecology* 81: 416–432.

Hopkinson, C.S., A.E. Giblin, J. Tucker, and R.H. Garritt. 1999. Benthic metabolism and nutrient cycling along an estuarine salinity gradient. *Estuaries* 22: 825–843.

Hou, L.J., M. Liu, H.Y. Jiang, S.Y. Xu, D.N. Ou, Q.M. Liu, and B.L. Zhang. 2003. Ammonium adsorption by tidal flat surface sediments from the Yangtze Estuary. *Environmental Geology* 45: 72–78.

Howarth, R.W. 1988. Nutrient limitation of net primary production in marine ecosystems. *Annual Review of Ecology* 19: 89–110.

Joye, S.B., and J.T. Hollibaugh. 1995. Influence of sulfide inhibition of nitrification on nitrogen regeneration in sediments. *Science* 270: 623–625.

Kristensen, E., and K. Hansen. 1999. Transport of carbon dioxide and ammonium in bioturbated (*Nereis diversicolor*) coastal, marine sediments. *Biogeochemistry* 45: 147–168.

Mackin, J.E., and R.C. Aller. 1984. Ammonium adsorption in marine sediments. *Limnology and Oceanography* 29: 250–257.

Magni, P., M. Shigeru, and K. Tada. 2002. Semidiurnal dynamics of salinity, nutrients and suspended particulate matter in an estuary in the Seto Inland Sea, Japan during a spring tide cycle. *Journal Oceanography* 58: 389–402.

Mondrup, T. 1999. Salinity effects on nitrogen dynamics in estuarine sediment investigated by a plug-flux method. *Biological Bulletin* 197: 287–288.

Morin, J., and J.W. Morse. 1999. Ammonium release from resuspended sediments in the Laguna Madre estuary. *Marine Chemistry* 65: 97–110.

Morlock, S., D. Taylor, A. Giblin, C. Hopkinson, and J. Tucker. 1997. Effect of salinity on the fate of inorganic nitrogen in sediments of the Parker River estuary, Massachusetts. *Biological Bulletin* 193: 290–292.

Mortimer, C.H. 1971. Chemical exchanges between sediments and water in the Great Lakes—Speculations on probable regulatory mechanisms. *Limnology and Oceanography* 16: 387–404.

Nielsen, L.P. 1992. Denitrification in sediment determined from nitrogen isotope pairing. *FEMS Microbiology Ecology* 86: 357–362.

Nixon, S.W. 1981. Remineralization and nutrient cycling in coastal marine ecosystems. In *Estuaries and Nutrients*, ed. B. J. Neilson and L. E. Cronin. Clifton: Humana.

Redfield, A.C. 1958. The biological control of chemical factors in the environment. *American Scientist* 46: 205–222.

Rivera-Monroy, V.H., and R.R. Twilley. 1996. The relative role of denitrification and immobilization in the fate of inorganic nitrogen in mangrove sediments. *Limnology and Oceanography* 41: 284–296.

Rosenfeld, J.K. 1979. Ammonium adsorption in nearshore anoxic sediments. *Limnology and Oceanography* 24: 356–364.

Rysgaard, S., P. Thastum, T. Dalsgaard, P.B. Christensen, and N.P. Sloth. 1999. Effects of salinity on NH_4^+ adsorption capacity, nitrification, and denitrification in Danish estuarine sediments. *Estuaries* 22: 21–30.

Seitzinger, S.P. 1988. Denitrification in freshwater and coastal marine ecosystems: Ecological and geochemical significance. *Limnology and Oceanography* 33: 702–724.

Seitzinger, S.P., W.S. Gardner, and A.K. Spratt. 1991. The effect of salinity on ammonium sorption in aquatic sediments: Implications for benthic nutrient cycling. *Estuaries* 14: 167–174.

Simon, N.S., and M.M. Kennedy. 1987. The distribution of nitrogen species and adsorption of ammonium in sediments from the tidal Potomac River and Estuary. *Estuarine, Coastal and Shelf Science* 25: 11–26.

Solorzano, L. 1969. Determination of ammonia in natural waters by the phenol hypochlorite method. *Limnology and Oceanography* 14: 799–801.

Sorensen, J., and B.B. Jørgensen. 1987. Early diagenesis in sediments from Danish coastal waters: Microbial activity and Mn–Fe–S geochemistry. *Geochimica et Cosmochimica Acta* 51: 1583–1590.

Strickland, J.D.H., and T.R. Parsons. 1972. *A practical handbook of sea-water analysis*, 2nd ed. Ottawa: Fisheries Research Board of Canada.

Thornton, S.F., and J. McManus. 1994. Application of organic carbon and nitrogen stable isotope and C/N ratios as source indicators of organic matter provenance in estuarine systems: Evidence from the Tay estuary, Scotland. *Estuarine, Coastal and Shelf Science* 38: 219–233.

Vallino, J.J., and C.S. Hopkinson. 1998. Estimation of dispersion and characteristic mixing times in Plum Island Sound Estuary. *Estuarine, Coastal and Shelf Science* 46: 333–350.

Weston, N.B., W.P. Porubsky, V.A. Samarkin, M. Erickson, S.E. MacAvoy, and S.B. Joye. 2006. Pore water stoichiometry of terminal metabolic products, sulfate, and dissolved organic carbon and nitrogen in estuarine intertidal creek-bank sediments. *Biogeochemistry* 77: 375–408.

Wright, R.T., R.B. Coffin, and M.E. Lebo. 1987. Dynamics of planktonic bacteria and heterotrophic microflagellates in the Parker Estuary, northern Massachusetts. *Continental Shelf Research* 7: 1383–1397.

Yin, K.D., and P.J. Harrison. 2000. Influences of flood and ebb tides on nutrient fluxes and chlorophyll on an intertidal flat. *Marine Ecology Progress Series* 196: 75–85.

Zimmerman, A.R., and R. Benner. 1994. Denitrification, nutrient regeneration and carbon mineralization in sediments of Galveston Bay, Texas, USA. *MEPS* 114: 275–28.